Decoherence in semiconductor nanostructures with type-II band alignment: All-optical measurements using Aharonov-Bohm excitons

I. L. Kuskovsky, L. G. Mourokh, B. Roy, H. Ji, S. Dhomkar, J. Ludwig, D. Smirnov, and M. C. Tamargo

Phys. Rev. B **95**, 165445 — Published 26 April 2017

DOI: 10.1103/PhysRevB.95.165445

Decoherence in semiconductor nanostructures with type-II band alignment: all-optical measurements using Aharonov-Bohm excitons

I. L. Kuskovsky,[1,3] L. G. Mourokh, [1,3] B. Roy, [1,3] H. Ji, [1,3] S. Dhomkar, [1,3] J. Ludwig,[4,5] D. Smirnov,[4,5] and M.C. Tamargo[2,3]

[1]Department of Physics, Queens College of CUNY, Flushing, NY 11367, USA

[2]Department of Chemistry, The City College of CUNY, New York, NY 10031, USA

[3]The Graduate Center of CUNY, New York, NY 10016, USA

[4]National High Magnetic Field Laboratory, Tallahassee, FL 32310, USA

[5]Department of Physics, Florida State University, Tallahassee, Florida 32306, USA

We examine the temperature dependence of the visibility of the excitonic Aharonov-Bohm peak in type-II quantum dots. We obtain a functional temperature dependence, which is similar to that determined by transport experiments, namely, with T^{-1} term due to electron-electron collisions and with T^{-3} term due to electron-phonon interactions. However, the magnitude of the latter term is much smaller than that for the transport electrons and similar to the interaction strength of the *exciton*-phonon coupling. Such suppressed electron-phonon interaction ushers a way for all-optical studies of decoherence processes in semiconductor nanostructures as other dephasing mechanisms become more pronounced.

Keywords: Aharonov-Bohm Effect, Quantum Decoherence, Type-II Quantum Dots

1. Introduction

Understanding the mechanisms of decoherence processes at the nanoscale has been a focus of research over the last 30 years. These studies are very important from a fundamental point of view, as such processes lead to a crossover between quantum and classical regimes, as well as due to the need to understand the behavior of modern nanoscale optoelectronic devices. For a long time, the main advances in this field have been associated with the observations of various quantum-mechanical phenomena in transport experiments in mesoscopic metals and semiconductors (e.g., [1, 2]), such as weak localization and anti-localization, universal conductance fluctuations, Aharonov-Bohm (AB) oscillations, and persistent currents. From these experiments, decoherence length (and time) can be extracted and compared to theoretical predictions.

According to the pioneering works [3, 4], the main decoherence mechanisms in mesoscopic systems are the electron-phonon (*e-ph*) and electron-electron (*ee*) interactions, with the temperature dependence of the inverse phase-breaking time given by

$$\tau_{\varphi}^{-1} = \tau_{ee}^{-1} + \tau_{eph}^{-1} = aT^{n} + bT^{3}, \qquad (1)$$

where generally $n = 2/3$ [3, 4] for nanowires and $n = 1$ for Aharonov-Bohm rings (e.g., refs. [5-7] and references therein) in the diffusive regime; in the ballistic one channel regime the dephasing length (and time) were shown to behave as T^{-1} (e.g., Refs. [8, 9]). In both cases the dephasing time is expected to diverge as $T \to 0$; however, in many actual experiments starting from Ref. [10] (for reviews, see Refs. [11, 12] and references wherein), the dephasing time *saturates* at very low temperatures.

In the present paper, we propose measurements of decoherence in semiconductors using a *contactless all-optical* experimental technique. Our studies are based on the excitonic Aharonov-Bohm effect (EABE) in type-II quantum dots (QDs). It was predicted that a nontrivial quantum phase can be acquired by an electric dipole moving in a magnetic field [13-16], and it can be observed via optical emission of radially polarized excitons in nanostructures with suitable ring-like geometry, such as quantum rings and

type-II disk-like QDs (e.g., [15-18]). EABE has been experimentally observed in a number of type-II QD systems by us and other groups, in quantum rings (Ref. [19] and references therein), as well as in type-I QDs with a suitable quantum well geometry [20]. Optical experiments are advantageous over conventional transport experiments for a number of reasons. First of all, they are contactless, so the account of contacts and contact configuration can be eliminated. Many efforts have been exerted previously to include contacts and their configurations in both analyses of experimental results and theoretical considerations [2, 5, 21-23]. Second, the EABE peak [24] is observed at a sufficiently large magnetic field (see Fig. 1 and discussion below), where the scattering on magnetic impurities, if any, is strongly suppressed [12, 25-27]. Third, as we show below, the inelastic interactions with phonons are much weaker for the light-excited electron-hole pairs than for the electrons participating in transport, so other dephasing mechanisms, such as pure dephasing and electron-impurity scattering, become more pronounced.

The rest of the paper is structured as follows. We present experimental data in Section 2. In Section 3, we examine theoretically the type-II exciton with weak electron-hole bonding and conclude that such system would *not* reproduce the observed features. Correspondingly, experimental results are discussed in Section 4 from the point of view of the strongly-bound model. The paper is summarized in Section 5.

2. Experimental Results

The samples studied are type-II ZnTe/ZnSe stacked submonolayer QDs grown using a combination of migration-enhanced epitaxy and molecular beam epitaxy (see Refs. [28-30] and references therein). The stacks are formed due to a strong vertical correlation between the quantum dot containing layers [31, 32]. The lateral separation between the QD stacks is much larger [33] than the size of the carrier orbit [34], allowing for the assumption that carriers orbit each stack independently. There are no magnetic impurities expected in these samples due to the nature of the growth procedure.

Magneto-photoluminescence (magneto-PL) measurements were performed at temperatures between 0.36 and 30 K with magnetic fields up to 18 T applied in the Faraday geometry using a high-field magneto-optical insert, as described in Ref. [35]. Light from a ThorLabs temperature-controlled 405 nm

laser diode was injected into a 365 μm fiber and delivered to the sample in a ^{3}He cryostat. Optical power density across the excitation spot was fixed to ~10 μW/cm^2. The collected photoluminescence (PL) was injected into a 550 μm fiber and delivered to a Princeton Instruments IsoPlane single grating spectrometer equipped with a thermoelectrically cooled CCD detector.

In Fig. 1 (a) we show PL spectrum at 5.5 K and zero magnetic field for one of the samples studied, whereas Fig. 1 (b) shows the corresponding magneto-PL up to 4 T for the same sample. This sample exhibits emission due to QDs only (see e.g., Refs. [30, 33] for PL from a set of samples that have both QD and isoelectronic bound exciton related emission), which allows for simple spectral integration. The result is shown in Fig. 1 (b). We note that the signal persists to above 27 K, indicating that the effect is very robust, which allows one to perform decoherence measurements by varying the temperature over two orders of magnitude. The peak (henceforth called the AB peak) at B_{AB} ~1.38 T is due to EABE [36]. We note that the exact position of the peak changes slightly with temperature for this sample; however, considering that we plot the AB transition from an integrated PL intensity rather than over specific spectral position, it is not unexpected, and does not affect the magnitude of the AB peak. The magnitude of the AB peak [30], counted from the minima for each curve as shown by the arrow in Fig. 1 (b) for the 0.3 K curve, and is plotted as a function of temperature in Fig. 2 (solid circles). The magnitude of the AB peak directly relates to the coherence of the carriers responsible for the optical emission.

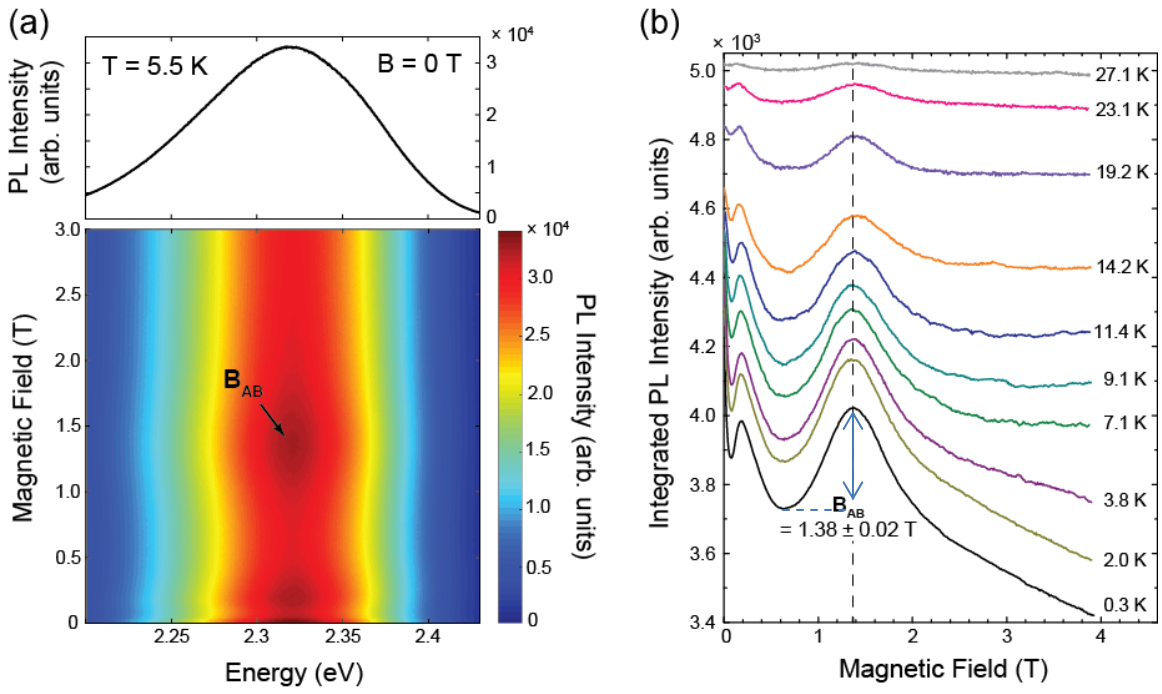

Figure 1 (a) Photoluminescence a sample with type-II QDs at zero magnetic field; **(b)** Magneto-PL of the same sample at the same temperature up to 4 T.; the peak at ~ 1.38 T is due to EABE; **(c)** Integrated PL as a function of magnetic field at different temperatures. Note: the plots are not shifted, but rather show actual experimental values.

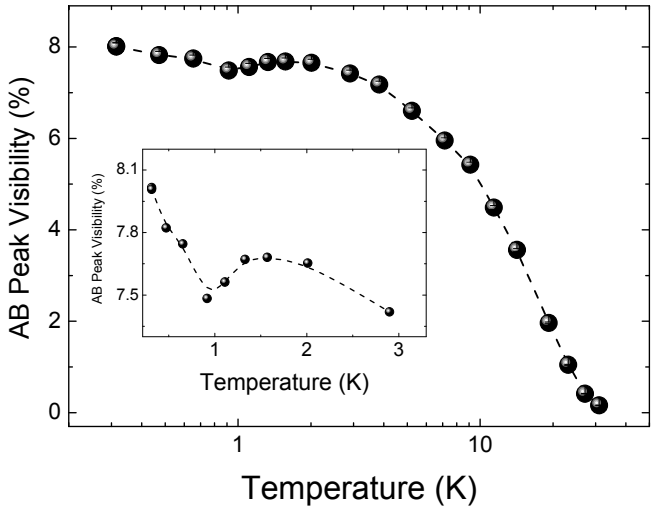

Figure 2 Magnitude of the AB 'peak' as a function of temperature. The dashed line is for eye guidance only.

3. Weakly- vs Strongly-Bound Exitons: Theoretical Examination

To further analyze the observed behavior, one needs to understand the type (strength) of the electron-hole interaction, which determines the character and shape of the optical Aharonov-Bohm peak., Two possible cases are discussed in Ref. [38]. For the weakly-bound exciton, when the electron and hole move independently, the exciton energy is given by

$$E_{exc}^{wb} = E_g^{wb} + E_e + E_h, \tag{2}$$

where E_g^{wb} is the magnetic-field-independent term,

$$E_e = \frac{\hbar^2}{2m_e R_e^2}\left(l_e + \frac{\Phi_e}{\Phi_0}\right)^2, \tag{3}$$

$$E_h = \frac{\hbar^2}{2m_h R_h^2}\left(l_h - \frac{\Phi_h}{\Phi_0}\right)^2, \tag{4}$$

$m_{e(h)}$ is the electron (hole) effective mass, $R_{e(h)}$ is the radius of the electron (hole) trajectory, $l_{e(h)}$ is the electron (hole) angular momentum, and $\Phi_{e(h)}$ is the magnetic flux through electron (hole) closed path loop. At zero magnetic field, the ground state is a bright state with (l_e, l_h) = (0, 0). With increasing magnetic field, eventually the dark state (l_e, l_h) = (-1, 0) becomes the ground one. However, for certain geometries, further increase of the magnetic field can make the ground state to be bright with (l_e, l_h)= (-1, +1) and dark again with (l_e, l_h)= (-2, +1). In this case, the enhancement of the luminescence is caused by the reappearance of the bright exciton. The corresponding luminescence peak position, width, and shape are determined mainly by the system geometry. Moreover, the second peak associated with the bright state (l_e, l_h) = (-2, +2) can occur.

For the tightly-bound exciton, when the electron and hole move together, the exciton energy is given by

$$E_{exc}^{tb} = E_g^{tb} + E_{e-h}, \tag{5}$$

where E_g^{tb} is the magnetic-field-independent term, and

$$E_{e-h} = \frac{\hbar^2}{2MR_0^2}\left(L + \frac{\Delta\Phi}{\Phi_0}\right)^2, \tag{6}$$

$R_0 = (R_e + R_h)/2$, $M = (m_e R_e^2 + m_h R_h^2)/R_0^2$, $L = l_e + l_h$, and $\Delta\Phi$ is the net magnetic flux through the area between the electron and hole trajectories. With such strongly correlated motion, the ground-state momentum only increases with magnetic field and the bright state cannot reappear. In this case the luminescence can be enhanced when the energies of the states with $L = 0$ and $L = +1$ become degenerated. In the ideal situation, there is just the level crossing. However, in reality, these states can be mixed (in particular, via the spin-orbit interaction) leading to the appearance of the two partially-bright states and possible enhancement of the luminescence. The experimentally obtained position of the peak does not allow one to choose one model vs the other. However, the predictions for a peak width and its shape are very different for each model.

For the case of the weakly-bound exciton, the magnitude of the peak can be affected by temperature via thermal broadenings of the levels. The temperature dependence of the visibility can be estimated from the contributions of the bright exciton populations. If the populations of the electron and hole levels are proportional to the Boltzmann factors, as

$$N_i^{e,h} \propto \exp\left\{-\frac{E_i^{e,h}}{k_B T}\right\}, \tag{7}$$

where $E_i^{e,h}$ are the electron and hole energies from Eqs. (3, 4) with angular momenta $i = 0, \pm1, \pm2, \ldots$, then the luminescence intensity is given by

$$I = \frac{\sum N_i^e N_{-i}^h}{\sum N_i^e \sum N_i^h}. \qquad (8)$$

The dependence of this intensity on the applied magnetic field is shown in Fig. 3 for various temperatures.

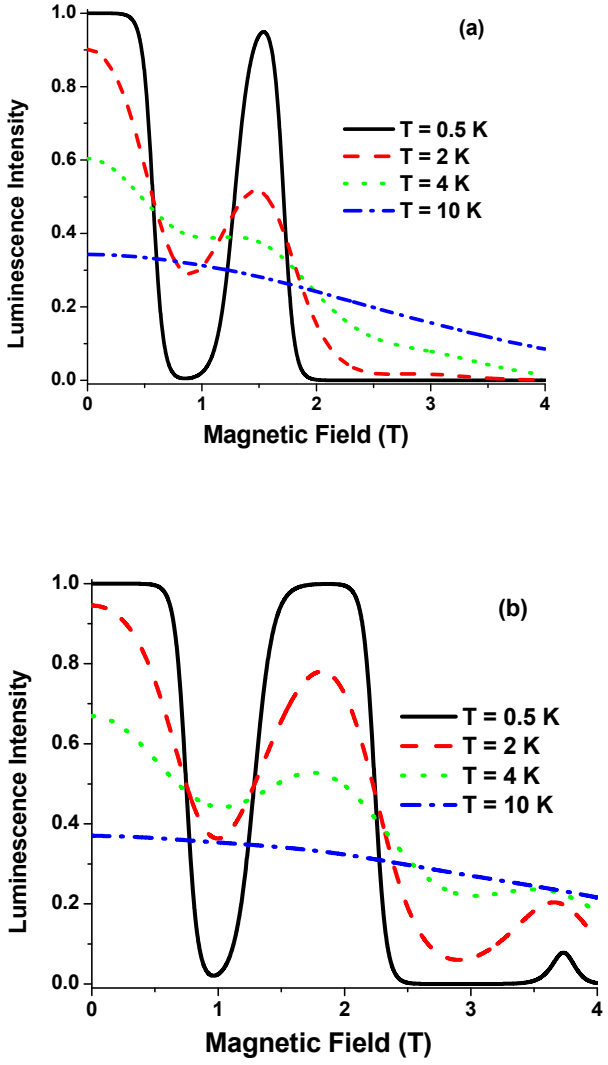

Figure 3 Calculated relative intensity of the luminescence as a function of magnetic field for various temperatures in the case of weakly-bound excitons. (a) R_h = 16 nm, R_e = 24 nm; (b) R_h = 16 nm, R_e = 21 nm

It is evident from this figure that the width and shape of the peak differ drastically from the experiment. Moreover, slight change of the system parameters can lead to the appearance of the second peak, as can be seen from Fig. 3 (b). The samples are evidently different from each other; nevertheless we have not observed a clear peak at the double magnetic field value at lower temperatures. The corresponding temperature dependence of the visibility is shown in Fig. 4. One can see that while the magnitude of the peak is indeed goes down with temperature as a result of thermal broadening, the functional dependence is completely different from the experimental results, Fig. 2.

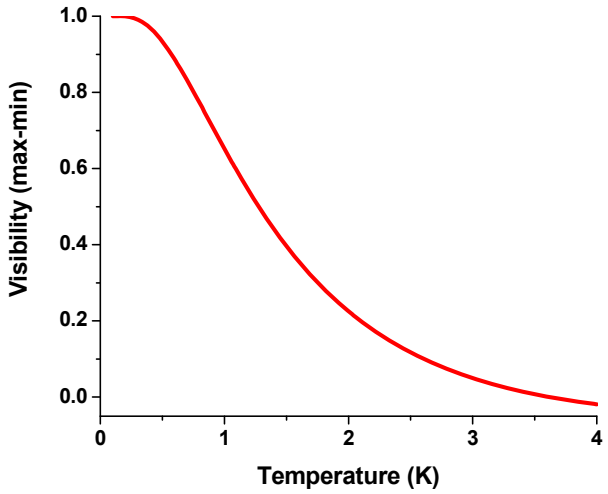

Figure 4 Calculated temperature dependence of the visibility in the case of weakly-bound excitons.

Moreover, the peak completely disappears above 4 K, which is in complete contradiction to our observations.

All these facts allow us to rule out the model of the weakly-bound [independent] electron-hole pair for our structures. For the tightly-bound excitons, thermal broadening would not affect the peak magnitude, although can be responsible for the initial luminescence suppression with increasing of the magnetic field. The arguments based on the comparison of the observed AB exciton size and the free excitons in ZnSe and ZnTe also led to the tight-binding model [37]. Moreover, we point to recent high

resolution x-ray diffraction (HRXRD) measurements on the same sample [32] that gave the average size of these QDs of 16 to 23 nm in radius, in excellent agreement with the tight-binding model [37].

4. Discussion

We thus believe that the temperature effects on the visibility are produced by the loss of coherence, i.e. by the destruction of the states with a well-defined angular momentum. In our model, therefore, while an electron and a hole are strongly coupled to form an exciton [33, 37], the electron travels over longer distances outside of the dot than the confined hole and its probability to be scattered is much larger. Correspondingly, the magnitude of the AB peak decreases exponentially with the electron path length D, similar to the amplitude of the AB oscillations observed in transport measurements (e.g., Ref. [9, 39] and references therein): $\Delta I_{AB} \propto exp[-D/D_\varphi]$, where D_φ is the coherence length. We also assume here that the ballistic regime applies, so that $D_\varphi \propto \tau_\varphi$. Indeed, as stated above, the lateral electron trajectory radius, R_{QD}, of the dots in all of our samples, is between 15 and 30 nm [34, 37], resulting in the electron path around the QD stacks, $2\pi R_{QD}$, between 100 and 200 nm. Thus, for further analyses we assume,

$$\Delta I_{AB} \propto \exp\left[-\frac{t_0}{\tau_\varphi}\right], \tag{9}$$

where t_0 is the time an exciton 'spends' on the orbit before recombining *either radiatively or non-radiatively*, similar to the time an electron spends in an interferometer or an AB ring in transport experiments [7]. Therefore, the experimental data are analyzed with the help of the following expression

$$\Delta I_{AB} = \Delta I_{AB}(0) \cdot exp[-At_0T - bt_0T^3]. \tag{10}$$

The result of fitting the experimental data to Eq. (10) is shown in Fig. 3 (red symbol-dotted line); the best fit was obtained for $At_0 = 0.04$ K^{-1} and $bt_0 = 9.2 \times 10^{-5}$ K^{-3}. The values for the other samples are shown in Table 1. We also show in Fig. 5 the separated best fits for the dependence of decoherence time

for low (T^{-1}) and high temperature (T^{-3}) cases. It is obvious that both the electron-electron- and electron-phonon-like scattering mechanisms must be included.

Next, we point out that in optical emission experiments, t_0 corresponds to the average lifetime of the electrons as measured by PL decay, and which accounts for both radiative and non-radiative recombinations. In our samples, within the temperature range of this experiment, the average PL lifetimes was determined to be between 50 and 100 ns [33]. This allows us to estimate $A = (4 \div 8) \times 10^{-4}$ $ns^{-1}K^{-1}$ and $b = (9.2 \div 18.4) \times 10^{-7}$ $ns^{-1}K^{-3}$. It should be emphasized that the value of parameter *b* here is much smaller than approximately 5×10^{-3} $ns^{-1}K^{-3}$ obtained after introducing ZnSe parameters into the corresponding expression in Ref. [40], where electron-phonon effects on decoherence were addressed. To further stress this point we estimate parameter *b* assuming that decoherence occurs via strictly non-radiative recommbination even though one would expect the quenching of the overall PL as well, which we do not observe. The non-radiative times estimated in Ref. [33] are of order 0.1 – 1 ns, would give parameter $b \sim 10^{-3}$ to 10^{-4}, which is still at least factor of 5 smaller.

We attribute smallness of parameter *b* to a strong electron-hole coupling due to an electrostatic interaction that cannot be neglected in type-II QDs [24]. Thus, even in the situation where only the electron is scattered, the whole electron-hole system emits or absorbs phonons, which diminishes such energy exchange. The situation here is similar to phonon scattering by donor-bound electrons considered by P. C. Kwok [41] for germanium. In our case, the confined hole plays the role of the positively charged donor. It was shown that the electron-phonon interaction is affected because of the discrete electron excitation spectrum. For the non-resonant case, the matrix element of the interaction can be calculated using second-order Born perturbation theory, i.e. it is strongly suppressed. We further note that parameter *b* is of the same order for all the samples we have measured, which indicates the material fundamental and sample-independent character of the exciton-phonon interaction.

Table 1

Sample	At_0 (K^{-1}), 10^{-2}	bt_0 (K^{-3}), 10^{-5}
D47	4	9.2
D51	2.9	2.5
D55	6.7	4.6

In Ref. [42], the temperature dependence of the excitonic dephasing rate was determined for temperatures from 5 to 120 K by means of the four wave mixing technique. The authors obtained a good fit using the predictions of the modified independent boson model [43] for the decoherence rate as

$$\gamma = \gamma_0 + \alpha T + b_1 \frac{1}{e^{E_1/k_B T} - 1} + b_2 \frac{1}{e^{E_2/k_B T} - 1}. \qquad (11)$$

Here E_1 and E_2 are the activation energies, with one of the energies (the larger one) being the optical phonon energy. The origin of the smaller energy was not well discussed and the possibility of pure dephasing was not excluded. We note that our attempt to fit our data using Eq. (11) resulted in two very similar values for the activation energy in the range of 2 to 6 meV, indicating that the interaction with optical phonons is not a decoherence mechanism for the AB excitons discussed here, in contrast to the results of Ref. [42], as expected for the temperature range, below 30 K, investigated here. Moreover, the α-parameter of Eq. (11) was determined to be zero in Ref. [42] indicating completely different functional temperature dependencies.

We attribute this difference to the fact that in type-I QDs of Ref. [42] both electrons and holes are confined, whereas in our type-II QD system electrons are mobile and thus scattered as in transport experiments. Correspondingly, we have to conclude that the phonon-induced dephasing in our system is due to *electron - acoustic-phonon* scattering, however, with diminished magnitude because of the strong electron-hole coupling [41].

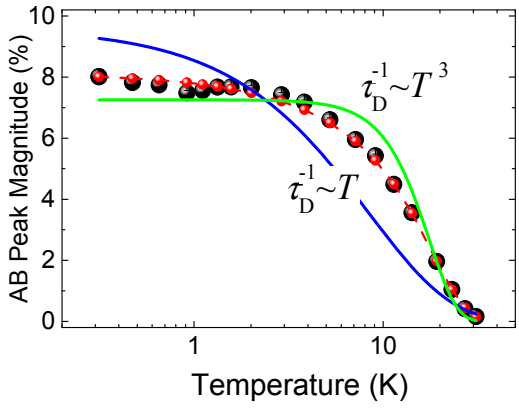

Figure 5 Magnitude of the AB 'peak' as a function of the temperature. The symbol-dashed line (red) is the fit to the functional dependence that accounts for electron-phonon and electron-electron scattering (Eq. (3))**.** Solid lines (green and blue) show dependencies arising from each mechanism, separately.

Finally, we comment on the low temperature data shown in the inset of Fig. 2, which indicate the existence of a minimum in the magnitude of the AB peak at around 1 K for this particular sample. We also observed smaller dips in other samples and somewhat different temperatures but within the same overall temperate range. The nature of this dip is not completely understood at this time, but it can be attributed to changes in the overall PL intensity observed from the samples. We plan to investigate it further, but we believe that it does not affect the overall temperature dependence of the AB peak presented in this work because our fitting covers a much larger temperature range than the dip vicinity.

5. Summary

In summary, we proposed a way to determine the temperature dependences of decoherence mechanisms based on an all-optical technique. The strength of the EABE was measured as a function of temperature over two orders of magnitude. We showed that at temperatures above 3 K, exciton-phonon scattering is the dominant cause of decoherence, and is the same for all samples. The obtained functional dependence on temperature is in agreement with that obtained in the electron transport experiments but the magnitude of the decoherence rate is much smaller confirming the benefits of the optical measurements.

The work is supported by the NSF under Award DMR-1006050 and the US Department of Energy Office of Basic Energy Sciences, Division of Materials Sciences and Engineering under Award DE-SC003739. Specifically, sample preparation was carried out with the DoE support (SD, MCT and ILK), while optical investigations were performed with support from the NSF (HJ and ILK). J.L. and D.S. acknowledge the support by NHMFL UCGP No. 5087. The work of L.M. is partially supported by AFOSR, Award No FA9550-16-1-0279. A portion of this work was performed at the National High Magnetic Field Laboratory, which is supported by National Science Foundation Cooperative Agreement No. DMR-1157490 and the State of Florida.

[1] Y. Imry, *Introduction to Mesoscopic Physics (Mesoscopic Physics and Nanotechnology, 2)* (Oxford University Press, USA, 2002), p. 256.

[2] T. Ihn, *Electronic Quantum Transport in Mesoscopic Semiconductor Structures* (Spinger-Verlag, New York, 2004), Vol. 192, p. 270.

[3] B. L. Altshuler, A. G. Aronov, and D. Khmelnitskii, J. Phys. C **15**, 7367 (1982).

[4] B. L. Altshuler, and A. G. Aronov, in *Electron-electron Interaction in Disordered Systems*, edited by A. L. Efros, and M. Pollak (North Holland, Amsterdam, 1985), p. p.1.

[5] T. Capron, C. Texier, G. Montambaux, D. Mailly, A. D. Wieck, and L. Saminadayar, Phys. Rev. B **87**, 041307 (2013).

[6] T. Ludwig, and A. D. Mirlin, Phys. Rev. B **69**, 193306 (2004).

[7] T. Ihn, *Semiconductor Nanostructures: Quantum State and Electronic Transport* (Oxford University Press, New York, 2010), p. 552.

[8] G. Seelig, and M. Büttiker, Phys. Rev. B **64**, 245313 (2001).

[9] A. E. Hansen, A. Kristensen, S. Pedersen, C. B. Sørensen, and P. E. Lindelof, Phys. Rev. B **64**, 045327 (2001).

[10] P. Mohanty, E. M. Q. Jariwala, and R. A. Webb, Phys. Rev. Lett. **78**, 3366 (1997).

[11] J. J. Lin, and J. P. Bird, J. Phys.: Condens. Matter **14**, R501 (2002).

[12] L. Saminadayar, P. Mohanty, R. A. Webb, P. Degiovanni, and C. Bäuerle, Physica E **40**, 12 (2007).

[13] M. Wilkens, Phys. Rev. Lett. **72**, 5 (1994).

[14] G. Spavieri, Phys. Rev. Lett. **82**, 3932 (1999).

[15] A. V. Chaplik, JETP Lett **62**, 900 (1995).

[16] A. B. Kalameitsev, V. M. Kovalev, and A. O. Govorov, JETP Lett. **68**, 669 (1998).

[17] R. A. Römer, and M. E. Raikh, Phys. Rev. B **62**, 7045 (2000).

[18] A. O. Govorov, S. E. Ulloa, K. Karrai, and R. J. Warburton, Phys. Rev. B **RC 66**, 081309 (2002).

[19] *Physics of Quantum Rings* (Springer, Berlin, 2014).

[20] L. Schweidenback, T. Ali, A. H. Russ, J. R. Murphy, A. N. Cartwright, A. Petrou, C. H. Li, M. K. Yakes, G. Kioseoglou, B. T. Jonker, and A. Govorov, Phys. Rev. B **85**, 245310 (2012).

[21] D. K. Ferry, S. M. Goodnick, and J. Bird, *Transport in Nanostructures* (Cambridge University Press, New York, 2009), p. 670.

[22] I. V. Lerner, B. L. L. Altshuler, and Y. Gefen, *Fundamental Problems of Mesoscopic Physics: Interactions and Decoherence* (Springer, New York, USA, 2004).

[23] Y. Murayama, *Mesoscopic Systems* (Wiley-VCH, Weinheim, Germany, 2001), p. 255.

[24] For type-II excitons that we study here, the Coloumb interaction is essential and cannot be considered small; thus, the case of 'weak confinement', according to classification by A. O. Govorov, S. E. Ulloa, K. Karrai, and R. J. Warburton, Phys. Rev. B RC **66**, 081309 (2002), is applied here. In this case only one AB peak is expected. See also discussion in Section 3.

[25] A. Benoît, D. Mailly, P. Perrier, and P. Nedellec, Superlattices Microstruct **11**, 3 (1992).

[26] F. Pierre, and N. O. Birge, Phys. Rev. Lett. **89**, 206804 (2002).

[27] P. Mohanty, and R. A. Webb, Phys. Rev. Lett. **91**, 066604 (2003).

[28] Y. Gu, I. L. Kuskovsky, M. van der Voort, G. F. Neumark, X. Zhou, and M. C. Tamargo, Phys. Rev. B **71**, 045340 (2005).

[29] I. L. Kuskovsky, W. MacDonald, A. O. Govorov, L. Mourokh, X. Wei, M. C. Tamargo, M. Tadic, and F. M. Peeters, Phys. Rev. B **76** 035342 (2007).

[30] B. Roy, H. Ji, S. Dhomkar, F. J. Cadieu, L. Peng, R. Moug, M. C. Tamargo, Y. Kim, D. Smirnov, and I. L. Kuskovsky, Phys. Rev. B **86**, 165310 (2012).

[31] S. Dhomkar, U. Manna, I. C. Noyan, M. C. Tamargo, and I. L. Kuskovsky, Appl. Phys. Lett. **103**, 181905 (2013).

[32] S. Dhomkar, N. Vaxelaire, H. Ji, V. Shuvayev, M. C. Tamargo, I. L. Kuskovsky, and I. C. Noyan, Appl. Phys. Lett. **107**, 251905 (2015).

[33] H. Ji, B. Roy, S. Dhomkar, R. T. Moug, M. C. Tamargo, A. Wang, and I. L. Kuskovsky, Journal of Elec Materi **42**, 3297 (2013).

[34] B. Roy, H. Ji, S. Dhomkar, F. J. Cadieu, L. Peng, R. Moug, M. C. Tamargo, and I. L. Kuskovsky, Appl. Phys. Lett. **100**, 213114 (2012).

[35] Y. Kim, Y. Ma, A. A. Imambekov, N. G. Kalugin, A. Lombardo, A. C. Ferrari, J. Kono, and D. Smirnov, Phys. Rev. B **85**, 121403(R) (2012).

[36] I. R. Sellers, I. L. Kuskovsky, A. O. Govorov, and B. D. McCombe, in *Physics of Quantum Rings*, edited by V. Fomin (Springer, Berlin, 2014), p. 487.

[37] H. Ji, S. Dhomkar, B. Roy, V. Shuvayev, V. Deligiannakis, M. C. Tamargo, J. Ludwig, D. Smirnov, A. Wang, and I. L. Kuskovsky, J. Appl. Phys. **116**, 164308 (2014).

[38] A. O. Govorov, S. E. Ulloa, K. Karrai, and R. J. Warburton, Phys. Rev. B **RC 66**, 081309 (2002).

[39] S. L. Ren, J. J. Heremans, C. K. Gaspe, S. Vijeyaragunathan, T. D. Mishima, and M. B. Santos, J. Phys.: Condens. Matter **25**, 435301 (2013).

[40] M. Y. Reizer, Phys. Rev. B **40**, 5411 (1989).

[41] P. C. Kwok, Phys. Rev. **149**, 666 (1966).

[42] P. Borri, W. Langbein, U. Woggon, V. Stavarache, D. Reuter, and A. D. Wieck, Phys. Rev. B **71**, 115328 (2005).

[43] B. Krummheuer, V. M. Axt, and T. Kuhn, Phys. Rev. B **65**, 195313 (2002).